doi:10.1017/S1431927622002628
Microsc. Microanal. 28 (Suppl 1), 2022

In-situ 4D-STEM of the Martensitic Phase Transformation in NiTi

Jennifer Donohue[1], and Andrew M. Minor[1,2,*]

[1.] Department of Materials Science and Engineering, UC Berkeley, Berkeley, CA, USA.
[2.] National Center for Electron Microscopy, Molecular Foundry, LBNL, Berkeley, CA, USA.
* Corresponding author: aminor@berkeley.edu

There is currently significant interest in new materials that exhibit large reversible strain responses to electric or magnetic fields because of their application in sensors and other devices. Materials which undergo displacive phase transformations can experience a large volume change on transformation. However, these responses are almost always accompanied by large hysteresis, limiting device applications. Theory states that the origin of this hysteresis is microscopic strain incompatibility at the interface of the parent and product phase. This strain incompatibility causes the accumulation of defects at the phase boundary [1-2]. Understanding how the nanoscale strain landscape develops at and before the transformation front in these materials is necessary to fully understand the origin of the high hysteresis in these systems. This understanding could be critical to the design of improved low-hysteresis materials with high recoverable strains. NiTi is a well-known example of a material which undergoes a displacive phase transformation and has critical industrial application, making an ideal model alloy for exploring the fundamental origins of this hysteretic behavior.

In this work, we use four-dimensional scanning transmission electron microscopy (4D-STEM) with high precision bullseye apertures [3] to map the nanoscale strain landscape during *in situ* cooling of a NiTi through the phase transformation from the high temperature B2 cubic austenite phase to the low temperature B19' monoclinic martensite phase. Using this method, we can map both the phase distribution and the strain as the sample approaches then proceeds through the phase transformation. In Figure 1 we demonstrate a map of the resulting structure at the transformation temperature 32C. Two distinct twinned martensite crystal diffraction patterns were observed and mapped (shown in red and blue). Some residual austenite (green) was also observed at the transformation temperature which allowed for the direct observation of the structural interface between the two phases. To understand the evolution of this structure before and after transformation, the development of strain along the $\langle 01\bar{1} \rangle$ direction of the B2 structure with reference to the lattice at 50C was mapped as shown in Figure 2(d-f). This mapping showed the expected decrease in spacing as the temperature is lowered with an interesting distribution of local strains before the transformation followed by the formation of the martensitic structure which shows a high deviation to the austenite lattice.

In addition to mapping strain, 4D-STEM is also used to visualize diffuse scattering during cooling as the sample approaches the phase transformation. Interestingly, we directly observe an increase in diffuse scattering as the temperature approaches the transformation temperature (see insets in Figure2 (a-c)). This is particularly interesting, as most materials upon cooling exhibit significantly reduced diffuse scattering around Bragg disks indicating reduced thermal vibrations. However, in NiTi as the temperature is reduced toward the transformation temperature, the diffuse scattering increases as the phase stability decreases. This phenomenon has been previously reported, however, there is considerable debate on the origin of this diffuse scattering. With this work, we aim to correlate the development of diffuse scattering, with the local strain landscape as a function of temperature through the transformation

temperature in NiTi. In addition, we correlate the resulting martensitic morphology with the precursor strain fields to reveal insight into the transformation dynamics in NiTi using *in situ* 4D-STEM [4].

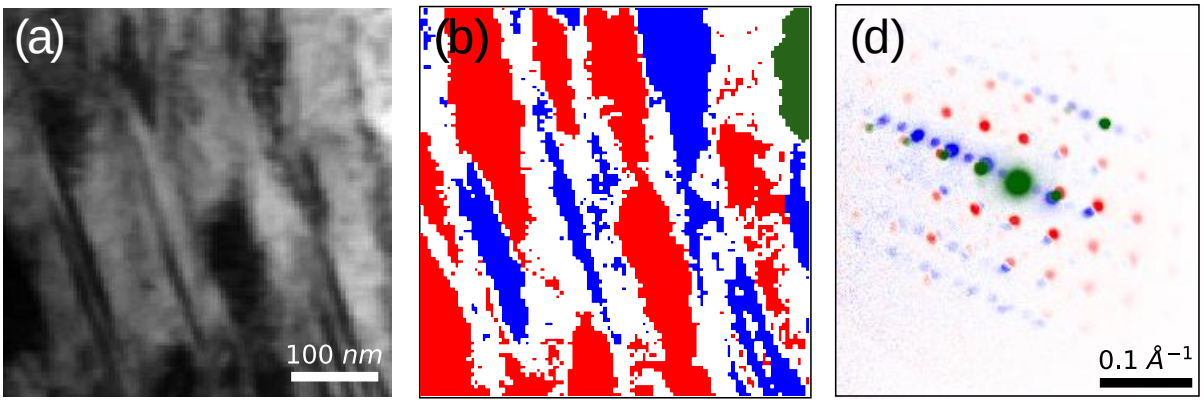

Figure 1. (a) virtual bright field image reconstructed from 4D-STEM data of NiTi at 32C, (b) phase map of NiTi at 32C with two B19' monoclinic martensite crystals (blue and red) as well as minimal residual cubic B2 austenite (green), and (c) overlaid mean diffraction patterns from each phase shown in (b)

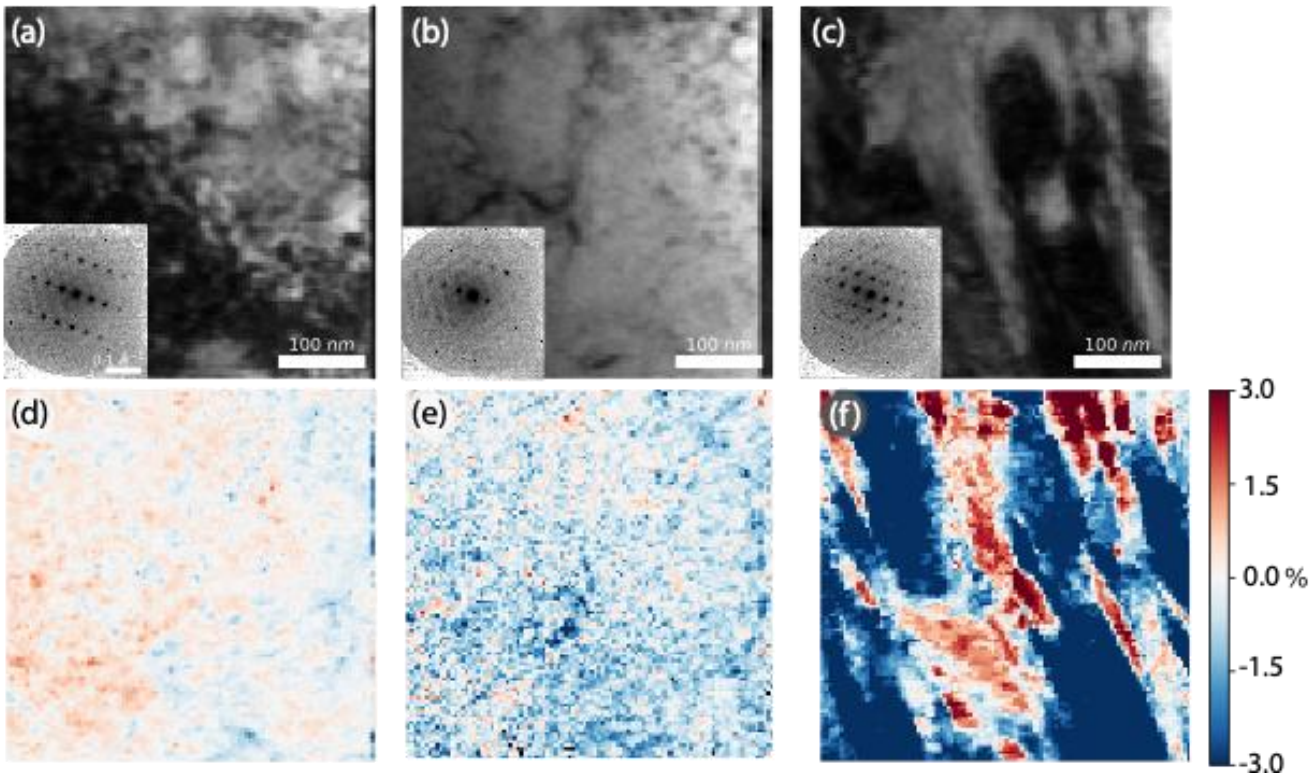

Figure 2. (a-c) virtual bright field images of NiTi with inset summed diffraction patterns reconstructed from 4D-STEM data acquired at 180C, 34C, and 30C respectively, (d-f) percent strain along the direction <$01\bar{1}$> of the B2 austenite NiTi structure with reference to the lattice at 50C

https://doi.org/10.1017/S1431927622002628 Published online by Cambridge University Press

References:

[1] Xu, Y. C. et al., Acta Materialia **171** (2019), p. 240-252. https://doi.org/10.1016/j.actamat.2019.04.027.
[2] Xu, YC. *et al*, npj Comput Mater **4(58)** (2018), p. 1-7. https://doi.org/10.1038/s41524-018-0114-7
[3] Zeltmann, S. E., et al. Ultramicroscopy, **209** (2020), a.112890. https://doi.org/10.1016/j.ultramic.2019.112890
[4] The authors acknowledge funding from the Department of Defense (DoD) through the National Defense Science and Engineering Graduate (NDSEG) Fellowship Program, and the National Science Foundation under STROBE Grant no. DMR 1548924. Work at the Molecular Foundry at Lawrence Berkeley National Laboratory was supported by the U.S. Department of Energy under Contract # DE-AC02-05CH11231.